Imperfect transparency and camouflage in glass frogs

James B. Barnett[a,b,1], Constantine Michalis[b], Hannah M. Anderson[a], Brendan L. McEwen[a], Justin Yeager[c], Jonathan N. Pruitt[a], Nicholas E. Scott-Samuel[d], and Innes C. Cuthill[b]

[a]Department of Psychology, Neuroscience & Behaviour, McMaster University, Hamilton, ON L8S 4K1, Canada; [b]School of Biological Sciences, University of Bristol, BS8 1TQ Bristol, United Kingdom; [c]Biodiversidad Medio Ambiente y Salud, Universidad de Las Américas, 170125 Quito, Ecuador; and [d]School of Psychological Science, University of Bristol, BS8 1TU Bristol, United Kingdom

Edited by Michael J. Ryan, University of Texas, Austin, TX, and accepted by Editorial Board Member James A. Estes April 17, 2020 (received for review November 7, 2019)

Camouflage patterns prevent detection and/or recognition by matching the background, disrupting edges, or mimicking particular background features. In variable habitats, however, a single pattern cannot match all available sites all of the time, and efficacy may therefore be reduced. Active color change provides an alternative where coloration can be altered to match local conditions, but again efficacy may be limited by the speed of change and range of patterns available. Transparency, on the other hand, creates high-fidelity camouflage that changes instantaneously to match any substrate but is potentially compromised in terrestrial environments where image distortion may be more obvious than in water. Glass frogs are one example of terrestrial transparency and are well known for their transparent ventral skin through which their bones, intestines, and beating hearts can be seen. However, sparse dorsal pigmentation means that these frogs are better described as translucent. To investigate whether this imperfect transparency acts as camouflage, we used in situ behavioral trials, visual modeling, and laboratory psychophysics. We found that the perceived luminance of the frogs changed depending on the immediate background, lowering detectability and increasing survival when compared to opaque frogs. Moreover, this change was greatest for the legs, which surround the body at rest and create a diffuse transition from background to frog luminance rather than a sharp, highly salient edge. This passive change in luminance, without significant modification of hue, suggests a camouflage strategy, "edge diffusion," distinct from both transparency and active color change.

camouflage | color change | edge diffusion | glass frog | transparency

Camouflage renders the visible invisible, or unrecognizable, with color patterns that blend into the background and/or disguise distinctive features (1, 2). Matching visually complex or heterogeneous backgrounds, however, demands compromise, and so many animals have developed ways of adapting their coloring to match the local conditions (3). Yet changing color is still limited by the range of pigments that can be produced, the pattern resolution (i.e., chromatophore density), and the speed with which pigments can be moved or synthesized (3, 4). Thus, rather than attempting to mirror the background, a better strategy may be to act as a window through which the background itself can be seen (5, 6).

Transparency is one of the most intuitive mechanisms of camouflage, allowing for instantaneous, high-fidelity, background matching regardless of the visual environment (6–8). Achieving transparency, however, requires the modification of a suite of tissues and structures to maximize light transmission, reduce scattering (9), avoid surface reflection, and minimize image distortion (6, 10).

Among aquatic species, transparency is relatively common and is facilitated by a variety of environmental factors, including the similarity in refractive indices between water and animal tissue, and a limited need for ultraviolet (UV) protective pigments (6, 9). Despite direct evidence of survival benefits being rare, indirect effects suggest that transparency does indeed act as camouflage. In transparent *Daphnia* spp. (Daphniidae), increasing the size of the eye (an obligate opaque structure) increases the risk of predation, and in areas where predatory fish are present, eye size is significantly smaller than in fish-free environments (11, 12). Similarly, aquatic copepods reduce their expression of pigments when presented with predator cues (13), and the concentration of pigmentation is significantly lower in environments containing fish predators (14).

In contrast, on land camouflage via transparency has been suggested in only a few instances: namely certain lepidopterans, such as the glasswing butterflies (Nymphalidae) (15, 16), and the glass frogs (Centrolenidae) (17). Evidence is emerging that the transparent wings of these lepidopterans can decrease detectability compared to opaque wings and that avian predators are less likely to capture transparent-winged species (15, 16), although the pigmented wing edges and bright flash marks of certain species may reduce the efficacy of transparency (18). Conversely, despite glass frogs being well known for their transparent skin, through which the internal organs can be observed (7, 17), the camouflage hypothesis has been controversial, with doubts over 1) the efficacy of transparency in terrestrial environments and 2) the degree to which glass frogs can be described as transparent (6, 7).

In truth, whereas the ventral skin of glass frogs is often transparent, the dorsum is pigmented, albeit sparsely (7, 17). Thus, under natural conditions, unlike the truly transparent wing membranes of glasswing butterflies (15, 16, 19), these frogs would be better described as translucent. This raises the question: what good is the glass frog's imperfect glass?

Significance

Transparency is one of the most intuitive forms of camouflage, where predators see straight through their prey as if it were not there. Glass frogs are a classic example of animal transparency and are well known for their transparent ventral skin, through which the internal organs can be clearly seen. The efficacy of transparency on land, however, has been controversial. We found that under natural conditions these frogs are better described as translucent and that translucency acts as modifiable camouflage. Differences in the degree of translucency over the frog act to disguise the frog's outline and highlight the potential of "edge diffusion" as a form of camouflage, making glass frog camouflage distinct from both transparency and active color change.

Author contributions: J.B.B., C.M., J.Y., J.N.P., N.E.S.-S., and I.C.C. designed research; J.B.B., C.M., H.M.A., B.L.M., and J.Y. performed research; I.C.C. contributed new reagents/analytic tools; J.B.B. analyzed data; and J.B.B., J.N.P., N.E.S.-S., and I.C.C. wrote the paper.

The authors declare no competing interest.

This article is a PNAS Direct Submission. M.J.R. is a guest editor invited by the Editorial Board.

Data deposition: Data have been uploaded to the Bristol Research Data Repository and are available at https://data.bris.ac.uk/data/dataset/3qnujjtjg4v4z2cztb4h882hh3.

[1]To whom correspondence may be addressed. Email: barnettj@mcmaster.ca.

This article contains supporting information online at https://www.pnas.org/lookup/suppl/doi:10.1073/pnas.1919417117/-/DCSupplemental.

First published May 26, 2020.

Whereas the role of transparency in camouflage is much discussed, translucency has received comparatively little attention. Indeed, the few published studies on translucency show that it can be used to increase, rather than decrease, conspicuousness in lizards. These lizards (*Anolis* sp. Dactyloiodae & *Draco* sp. Agamidae) orientate their translucent dewlaps to be backlit by the sun so that the diffuse transmission of sunlight brightens their sexually selected signals (20, 21).

Here, we describe an alternative where translucency facilitates a form of camouflage distinct from transparency and active color change. We examined the extent of glass frog translucency using models of predator vision and assessed whether translucency affected the efficacy of camouflage through a computer-based detection experiment with human participants and an in situ predation study with the frog's wild predators (22, 23).

Results

Visual Modeling. We took calibrated photographs of 25 adult *Teratohyla midas* in French Guiana and 30 *Espadarana prosoblepon* in Ecuador. All frogs were photographed under natural daylight conditions on two backgrounds that differed in luminance and hue: dark green (fresh leaves) and bright white (Rite-in-the-Rain White All-Weather Copier Paper 8512-M, JL Darling). The photographs were taken with a Nikon digital single-lens reflex (DSLR) camera (*T. midas*, D3200; *E. prosoblepon*, D7200) and AF-S DX NIKKOR 35-mm prime lens (Nikon), and each contained a ColorChecker Passport (X-Rite) to enable color calibration and scaling. The frog's color on each background was then assessed using four visual models: tetrachromatic avian (24), trichromatic snake (25), dichromatic mammal (26), and trichromatic human (27, 28).

First, we quantified perceived color change by comparing the accuracy with which a generalized linear mixed-effects model [R package lme4 (29) in R 3.5.1 (30)] could discriminate between the frogs on the two backgrounds. The higher the classification accuracy, the greater the change between the backgrounds. Classification accuracy was characterized using the Area Under the Curve (AUC) of Receiver-Operated Characteristic (ROC) curves [R package pROC (31)], following this common grading system: 1.0 to 0.9 = excellent; 0.9 to 0.8 = good; 0.8 to 0.7 = fair; 0.7 to 0.6 = poor; and 0.6 to 0.5 = fail (32).

We found that, overall, each visual model was fair (*T. midas*) or poor (*E. prosoblepon*) at discriminating the frogs on the white background from the frogs on the leaves (Fig. 1 and *SI Appendix*, Tables S1 and S2). However, accuracy was not equal across all parts of the frogs: each model was either poor at detecting or failed to detect any change in luminance or hue from the body but was good at distinguishing the legs. This indicates that although the frog's body largely retained its appearance atop the two different backgrounds, the legs changed significantly. This change was largely the result of a shift in achromatic contrast rather than hue and, although the frogs' base color did not exactly match this sample of leaves, the perceived luminance shifted toward that of the immediate background (Fig. 1 and *SI Appendix*, Tables S1 and S2).

Detection. Second, to evaluate whether the changes described in the visual modeling could enhance camouflage, without the potential confound of neophobia, we ran an ex situ computer-based detection experiment with human participants. It is important to note the existence of differences in visual perception between species and to be cautious when applying human-derived data to other animals. There are, however, deep underlying similarities in visual processing between species (33), and many studies show a strong correspondence in what makes prey detectable between humans and wild avian predators (e.g., refs. 16, 27, 34, 35).

We created frog-shaped stimuli using a standardized template of *T. midas* in its diurnal resting posture. We extracted the mean luminance and hue of the body and the degree of translucency from the legs for each of the 25 *T. midas* used for the visual modeling. We then used these data to create treatments A through D where we manipulated the distribution of the translucent elements. Treatment E used the mean colors from randomly selected green leaves photographed in situ. This created five treatments: A—natural pattern: translucent legs and opaque body; B—reversed pattern: opaque legs and translucent body; C—fully translucent; D—fully opaque; and E—opaque leaf color. Twenty human participants were tasked with finding the frogs as quickly as possible against a background made up of calibrated photographs of green leaves. Reaction time (RT) was log-transformed and analyzed with a general linear mixed-effects model, and detection accuracy (DA) was analyzed with a binomial generalized mixed-effects model [R package lme4 (29) in R 3.5.1 (30)].

We found a significant effect of treatment on the time taken to detect the frogs ($\chi^2 = 831.20$; degrees of freedom (df) = 4; $P < 0.001$; Fig. 2, *Left* and *Middle*) and for detection accuracy ($\chi^2 = 430.41$; df = 4; $P < 0.001$). Pairwise tests of a priori interest [R package multcomp (36)] showed that the natural pattern was significantly harder to detect than the entirely opaque frog (A to D: RT z = 2.95; $P = 0.012$; DA z = 0.34; $P = 0.991$) and that there was no significant difference between the three patterns that included translucent elements (A to B: RT z = 1.26; $P = 0.542$; DA z = 0.11; $P = 1.00$; A to C: RT z = 0.98; $P = 0.733$; DA z = 0.99; $P = 0.718$). In line with the visual modeling, we also found that the frog's opaque base color was detected significantly more quickly and accurately than the opaque background sample (D to E: RT z = −26.75; $P < 0.001$; DA z = 13.72; $P < 0.001$).

Survival. Finally, to test whether these effects corresponded to survival advantages under natural conditions, we ran an in situ predation study with model frogs and wild predators in Ecuador. We used green gelatin to create two treatments: translucent and opaque ($n = 180$ per treatment). These models were placed on vegetation, in 19 independent blocks, along riparian transects. Over the course of 72 h, we recorded how quickly each treatment was predated by wild predators (mainly birds, based on the frequent presence of beak marks), and we analyzed mortality with a mixed-effects Cox model [R package coxme (37)]. We found a significant effect of treatment ($\chi^2 = 14.81$; df = 1; $P < 0.001$) and that translucent models had a significantly lower mortality rate than opaque frogs (z = −3.70; $P < 0.001$; Fig. 2, *Right*).

Discussion

Taken together, our data suggest that glass frog translucency does act to provide ecologically relevant camouflage. We found that, without any changes in pigmentation, the perceived luminance of the frogs changed depending on the background, making each frog a closer match to its immediate surroundings. Unlike true transparency, however, color change was largely restricted to luminance rather than hue. The frogs therefore appeared green at all times but seemed to brighten and darken depending on the substrate against which they were viewed. We further found that this translucency resulted in glass frogs being more difficult for human participants to detect and less likely to be attacked by wild predators than opaque frogs.

Being transparent, like the membranous wings of glasswing butterflies, allows whole background structures to be visible through the organism (15, 16). Translucent glass frogs, on the other hand, retain their green hue regardless of the background, and background patterning does not show through the frog. The glass frogs' natural history does, however, provide a means to bridge the potential efficacy gap between translucency and transparency. Under natural conditions glass frogs remain stationary during daylight hours, resting flat against leaves, with their legs tucked to the sides of their body. By resting

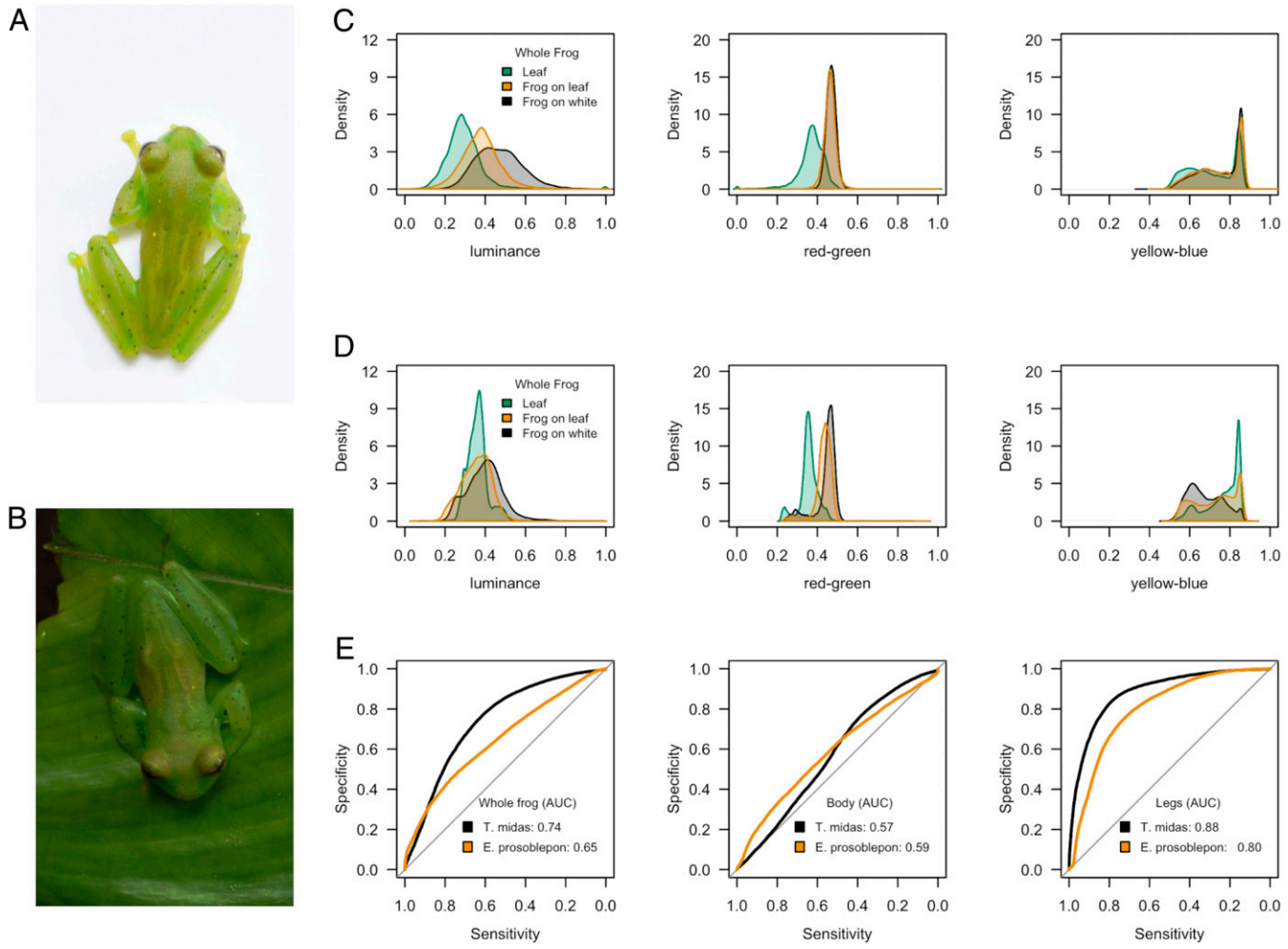

Fig. 1. Visual modeling of color change (avian visual model). (*A*) *E. prosoblepon* on the white background. (*B*) *E. prosoblepon* on the leaf background. (*C* and *D*) *T. midas* and *E. prosoblepon*, respectively: the response of each channel of the avian visual model to the leaf background (green), the whole frog on the leaf (orange), and the whole frog on the white background (black). The frog's luminance, more so than its hue, shifts toward that of the immediate background. (*E*) ROC curves from the avian visual model for the whole frog (*Left*), the frog's body (*Middle*), and the frog's legs (*Right*) for both species' color change was strongest on the frog's legs. AUC: 0.5 to 0.6 = fail; 0.6 to 0.7 = poor; 0.7 to 0.8 = fair; 0.8 to 0.9 = good; and 0.9 to 1.0 = excellent.

predominantly on living green leaves, the frogs' natural background does not include complex visual textures and will vary much more in luminance than hue.

This limits the necessity for more dramatic changes in hue, reduces the need for dynamic pattern matching, and allows the frogs' green pigmentation to act as generalist background-matching camouflage. This generalist base color is then calibrated by diffuse light transmission to increase camouflage passively against the immediate background. This camouflaging effect would apply to both diurnal and nocturnal predators and was consistent across a diverse range of potential predator visual systems that differ greatly in color perception. Translucency, therefore, allows perceived luminance to change while continuing to allow pigmentation to screen any obligate opaque structures (e.g., thick or complex body tissues) from view and, potentially, from harmful UV radiation.

Moreover, the change in perceived luminance was greater on the frogs' legs than on the body, which remained principally the same brightness regardless of the background. As such, when at rest and the relatively opaque body is surrounded by the more translucent legs, the frog becomes a diffuse gradient from substrate to dorsal color rather than producing a sharp, high-contrast outline. Visual systems are particularly sensitive to high-contrast edges, especially in the luminance domain (33, 38), and low-intensity, graduated boundaries have been demonstrated to make artificial camouflaged targets more difficult to detect (39).

Camouflage strategies are defined by the perceptual processes that the pattern exploits rather than the features of the pattern per se (2). Transparency is most frequently considered to produce a form of camouflage akin to background matching, with the transparent animal blending into its immediate surroundings (6). Transparency and translucency, however, may also facilitate other defensive strategies. Many species of clearwing moths (e.g., Sesiidae, Lepidoptera) are Batesian mimics, and their transparent wings match those of venomous wasps (e.g., Vespidae, Hymenoptera). Similarly, many species of katydid (Tettigonidae, Orthoptera) and leaf insect (Phyllidae, Phasmatodea) masquerade as leaves with incredibly precise mimicry that often includes translucent elements representative of leaf damage.

Furthermore, the irregular translucent elements found on the otherwise opaque wings of many moths may act as disruptive camouflage, with translucent components blending into the background to leave unrecognizable false edges (34, 40). The "edge diffusion" observed in glass frogs represents a form of camouflage conceptually linked with disruptive coloration (41),

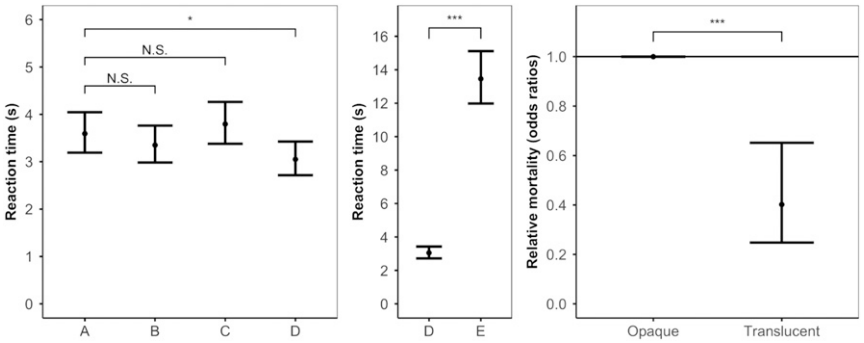

Fig. 2. Reaction time and relative mortality. (*Left*) Time taken for human participants to find frogs with different levels of translucency (means and 95% CI): stimuli using the base color of *T. midas*: A—natural pattern, translucent legs, and opaque body; B—reverse pattern, opaque legs, and translucent body; C—fully translucent; D—fully opaque. There was no significant difference between the natural pattern and frogs with some level of translucency (A to B and A to C), but the frog's natural level of translucency was significantly harder to detect than a fully opaque frog (A to D: * represents $P = 0.012$). (*Middle*) Comparison between the mean color of each frog's body (D) to random sample background matching (E). The frogs' mean colors did not match the background (Fig. 1), and random sample background matching was significantly harder to detect than the mean color of each frog (D to E: *** represents $P < 0.001$). (*Right*) Predation rate of model frogs (odds ratios with 95% CI in relation to the opaque frog). The translucent frog had a significantly lower mortality rate (higher survival) than the opaque frog (*** represents $P < 0.001$).

but whereas disruption reduces the relative contrast of the target's outline, edge diffusion reduces the absolute intensity of the edge.

As such, the translucent appearance of many glass frogs acts to provide camouflage in a manner conceptually distinct from both true transparency and active color change. Rather than allowing the background to be directly seen, diffuse light transmission through the frog adjusts a generalist camouflage pattern to more closely match the immediate background. This change in perceived luminance then transforms the frogs' salient high-intensity outline into a less conspicuous graduated boundary. Thus, the imperfect glass of the glass frog provides effective camouflage, disguising the frogs' outline and blending the frog and the leaf more smoothly together.

Materials and Methods

Image Collection. *T. midas* ($n = 25$) were encountered in the rainforest surrounding the Saut-Pararé camp of the Nouragues Natural Reserve, French Guiana (December 2014 to January 2015), and *E. prosoblepon* ($n = 30$) were sampled along streams near the town of Mindo, Pichincha Province, Ecuador (May to July 2019). In order to assess the degree to which translucency produces color change, each frog was photographed on two backgrounds in a random order and in quick succession (to remove the influence of any change in pigmentation) on a sheet of white waterproof paper (Rite-in-the-Rain White All-Weather Copier Paper 8512-M, JL Darling), and fresh dark-green leaves that were collected from the same trees on which glass frogs were seen calling (Fig. 1). In addition, for the detection experiment we photographed 10 leaves from each of 10 tree species ($n = 100$) found in the same location as *T. midas* were observed to be calling.

Each frog, and each leaf, was photographed from directly above, under natural daylight conditions, with a Nikon DSLR camera (*T. midas*, D3200; *E. prosoblepon*, D7200) and AF-S DX NIKKOR 35-mm prime lens (Nikon). To enable color calibration and scaling, all images contained a ColorChecker Passport (X-Rite). Frogs were then released at the precise location from where they were collected.

Visual Modeling. Each photograph was linearized, size-scaled, and calibrated in accordance with the ColorChecker Passport (42). The pixels corresponding to the frog (both legs and body) and the background (white background vs. green leaf) were specified and saved separately in MATLAB 2018b (The MathWorks).

Image analysis used four visual models corresponding to three potential visual predators as well as human vision: tetrachromatic avian, trichromatic snake, dichromatic mammalian, and trichromatic human L*a*b* (27, 43, 44). Human vision was included to allow intuitive interpretation of visual and detection data. Humans are trichromatic, with peak absorption (λ_{max}) of 564 nm (longwave sensitive: LWS), 534 nm (mediumwave sensitive: MWS), and 420 nm (shortwave sensitive: SWS) (28). Human L*a*b* is an international standard color space derived from psychological testing (CIELAB, 1976); however, because an equivalent visual model for nonhuman species is not available, the avian, snake, and mammalian models used relative cone capture rates.

Cone capture rates were used to generate a three-dimensional (3D) color space which categorized perceivable colors along orthogonal opponent channels in a similar manner to L*a*b*: luminance (L) and the opponent channels red-green (rg) and yellow-blue (yb). Although opponent processes have not been characterized for the nonhuman visual systems that we model, these orthogonal color channels represent an efficient way to encode visual information and, as such, a biologically plausible estimate of visual contrast (45).

To check for UV reflectance, we photographed *E. prosoblepon* under natural daylight conditions with a UV-sensitive, full-spectrum quartz-converted Canon EOS 7D (Canon) and NIKKOR EL 80-mm lens (Nikon) as well as appropriate filters for human visible and infrared light. Each image contained two luminance standards to enable calibration: 77% and 10% reflectance (Labsphere). UV irradiance is low below the forest canopy, and we found there to be little UV reflectance from either the frog or its background (*SI Appendix*, Fig. S1). Consequently, the UV channel did not contain any information and was excluded from our visual models (27). The mammalian visual model lacks an MWS cone and so was modeled in two dimensions: L and yb (27, 35, 43).

The avian model used the violet-sensitive tetrachromatic vision of the Indian peafowl (*Pavo cristatus* Galliformes) with λ_{max} at 605 nm (LWS), 537 nm (MWS), 477 nm (SWS), 432 nm (VS), and luminance-measuring double cones at 567 nm (D) (24). L was generated from the response of the D cone, rg was the relative stimulation of the LWS to MWS cone, and yb was the relative stimulation of the LWS and MWS to the SWS cone.

The snake model used the UV-sensitive trichromatic vision of the whip snake (*Masticophis flagellum* Colubridae) with λ_{max} at 561 nm (LWS), 458 nm (MWS), and 362 nm (UV) (25). L was calculated from the stimulation of the LWS cone, rg from the relative stimulation of the LWS to MWS cone, and yb from the combined stimulation of the LWS and MWS to the UV cone.

The mammalian model used the dichromatic vision of the domestic ferret (*Mustela putorius* Mustelidae) with λ_{max} of 558 nm (LWS) and 430 nm (SWS) (26). L was calculated from the LWS cone, and yb was the ratio of the LWS to the SWS.

Image Analysis. Chromatic information was analyzed using a generalized linear mixed-effects model [R package lme4 (29) in R 3.5.1 (30)]. Our approach has parallels with the Vorobyev and Osorio receptor-noise–limited model (46), but rather than comparing pairs of pixels, we were interested in determining the separability of two clouds of points within the color space. To avoid overfitting, we used leave-one-out cross validation (32), the unit of omission being the frog rather than the pixel (27). The degree of color change was quantified as the discrimination accuracy between the frog on the white background and the frog on the leaf using the AUC of ROC curves [R package pROC (31)]. The AUC represents the probability of correct identification with 1.0 indicating perfect discrimination and 0.5 indicating chance. We followed a common grading system: 1.0 to 0.9 = excellent; 0.9 to

0.8 = good; 0.8 to 0.7 = fair; 0.7 to 0.6 = poor; and 0.6 to 0.5 = fail (27, 32). The higher the AUC, the greater the change between the two backgrounds.

Detection Stimuli. To create the experimental backgrounds, each leaf photograph (n = 100) was calibrated in accordance with the ColorChecker Passport (42), and the whole leaf was cropped from the image and saved separately using MATLAB 2018b. The experimental backgrounds were generated by layering all 100 leaves in a random sequence, with leaf orientation and position randomly selected.

For the frog stimuli, we used the colors of the 25 *T. midas* photographed for the visual modeling and a standardized template in the shape of *T. midas* in a diurnal resting posture, flat to the leaf with its legs to the side of its body. As the color of the frogs' bodies did not change significantly between backgrounds, we calculated the mean color of each frog's body and used these as the base colors for the experimental stimuli.

We manipulated frog color to generate five treatments. Treatments A, B, C, and D used the mean colors of the frogs: A was a frog with translucent legs and an opaque body (as found in the natural condition); B had a translucent body and opaque legs (reverse of the natural condition); C was a frog with a translucent body and translucent legs; D was an opaque frog; and E represented random sample background matching where each replicate was an opaque frog with the mean color of a randomly selected leaf.

Translucency was simulated by modifying the alpha data of the frog image file (opaque $\alpha = 1.00$; translucent $\alpha = 0.85$) in MATLAB 2018b. The ecological validity of the approach was assessed by repeating the visual modeling protocol on the experimental stimuli. We generated stimuli using the mean colors of each of the 25 frogs and translucency (α) values set at 5% increments between 100% (opaque) and 75% (translucent). Each stimulus was digitally rendered both against a white background and on the experimental (leaf) backgrounds. One thousand pixels corresponding to the target area were then randomly selected, extracted, and converted into L*a*b* color space. We ran a generalized linear mixed-effects model with leave-one-out cross validation using the mean human L*a*b* model responses for each frog. We compared the frog color between the two backgrounds for each level of transparency, as well as for the mean color for the real frogs' legs on the white and leaf backgrounds. We found that an α of 0.85 resulted in a degree of color change (AUC) that most closely matched the legs of *T. midas* (AUC: frog legs = 0.95; α 100% = 0.53; α 95% = 0.74; α 90% = 0.85; α 85% = 0.97; α 80% = 1.00; α 75% = 1.00), and so we defined α as 0.85 in the detection experiment.

Detection Protocol. Each participant (n = 20, with normal or corrected to normal vision) was presented the five stimuli generated from each of the 25 frogs (n = 125) on a 13-inch MacBook Air (Apple). Each frog was paired with a uniquely generated background and was placed at a random location with a randomly selected rotation. Each participant therefore saw a unique set of frog-background combinations, and these stimuli were presented in a separately randomized sequence (*SI Appendix*, Fig. S2). We recorded reaction time and detection accuracy, with all clicks within a circle centered on the frog with a diameter equal to the frog's length, classified as correct.

Detection Analysis. Reaction time was log-transformed and analyzed with a general linear mixed-effects model, and detection accuracy was analyzed with a binomial generalized mixed-effects model [R package lme4 (29)]. Pairwise comparisons, of a priori interest, were designed to test particular hypotheses [R package multcomp (36)]. We compared treatment A to treatments B, C, and D to assess whether the amount and distribution of translucency affected detectability, and treatment D to E to test whether the frogs' pigmented color was as successful as random sample background matching. As the number of comparisons is equal to the number of degrees of freedom, P values were not adjusted.

Survival Protocol. The survival experiment was conducted along riparian transects near the town of Mindo (Pichincha Province, Ecuador), a site where the glass frog *E. prosoblepon* was common. We used a randomized block design with two treatments: translucent and opaque. The models were placed out in 19 independent blocks, containing 10 of each treatment, aside from blocks 12 and 13 which, due to damaged models, each contained 5 of each treatment (n = 180/treatment). Models were tied to green leaves along each transect spaced apart as to be independent of one another. Evidence of predation was recorded at 24, 48, and 72 h after the block was placed out. Relative mortality was assessed with a mixed effects Cox model [R package coxme (37)], with evidence of predation recorded as full events and missing, rain damaged, or surviving models recorded as censored values.

Model frogs were made from a mixture of water and unflavored sugar-free gelatin powder (Supermaxi, Corporación Favorita). The solution naturally dried translucent with a slight yellow tint, and so we added a small amount of corn starch to modify opacity, and green food coloring (La Reposterita) to control color. To make 12 frogs, we first added the food coloring (translucent = 0.05 mL; opaque = 0.10 mL) to 380 mL of boiling water. We then mixed 56 mL of green boiling water into 15 g of gelatin powder plus a small amount of corn starch (translucent = 0.20 g; opaque = 0.50 g). The solution was then poured into a silicone mold (Alumilite Amazing Mold Rubber) created using a 3D print of a tree frog (*Phyllomedusa tomopterna*) in a resting posture (Digital Life Project, Department of Biology, University of Massachusetts Amherst), which was scaled to match the body length (25 mm) of *E. prosoblepon*. Models were left to solidify overnight and attached to leaves the following morning.

To assess whether the two treatments differed in opacity as viewed by potential predators, we replicated the image analysis protocol with the avian visual model (outlined above). We photographed the models (n = 5/treatment) on two backgrounds—white waterproof paper and a dark green leaf—under natural daylight conditions. Each image contained a ColorChecker Passport and was taken with a Nikon D7200 DSLR camera and AF-S DX NIKKOR 35-mm prime lens. Plotting the model response shows that hue (both red-green and yellow-blue) was similar between the two models and was largely stable across the two backgrounds. Perceived luminance, however, shifted depending on the background in a similar manner to the real frogs, such that the translucent models were a closer match to the background luminance (*SI Appendix*, Fig. S3).

Data Deposition. Raw data are available in the University of Bristol Research Data Repository (https://data.bris.ac.uk/data/dataset/3qnujjtjg4v4z2cztb4h882hh3).

ACKNOWLEDGMENTS. We thank the staff of CNRS and the Nouragues Natural Reserve (French Guiana). J.B.B. thanks Julia Barnett for help with image processing, and I.C.C. thanks the Wissenschaftskolleg zu Berlin for support during part of the study. We thank all members of the CamoLab (University of Bristol) and the J.N.P. Lab (McMaster University) for their help in discussion. This work was supported by CNRS Grant ANR-10-LABX-25-01 (to J.B.B., C.M., N.E.S.-S., and I.C.C.); Biotechnology and Biological Sciences Research Council Grant BB/S00873X/1 (to I.C.C.); Canada 150 Chair (J.N.P.); and Universidad de de Las Américas, Quito, Ecuador Grant FGE.JY.19.04 (to J.Y.).

1. I. C. Cuthill *et al.*, The biology of color. *Science* **357**, eaan0221 (2017).
2. I. C. Cuthill, Camouflage. *J. Zool. (Lond.)* **308**, 75–92 (2019).
3. R. C. Duarte, A. A. V. Flores, M. Stevens, Camouflage through colour change: Mechanisms, adaptive value and ecological significance. *Philos. Trans. R. Soc. Lond. B Biol. Sci.* **372**, 20160342 (2017).
4. M. Stevens, Color change, phenotypic plasticity, and camouflage. *Front. Ecol. Evol.* **4**, 51 (2016).
5. A. I. Houston, M. Stevens, I. C. Cuthill, Animal camouflage: Compromise or specialize in a 2 patch-type environment? *Behav. Ecol.* **18**, 769–775 (2007).
6. S. Johnsen, Hidden in plain sight: The ecology and physiology of organismal transparency. *Biol. Bull.* **201**, 301–318 (2001).
7. M. J. McFall-Ngai, Crypsis in the pelagic environment. *Am. Zool.* **30**, 175–188 (1990).
8. L. E. Bagge, Not as clear as it may appear: Challenges associated with transparent camouflage in the ocean. *Integr. Comp. Biol.* **59**, 1653–1663 (2019).
9. S. Johnsen, Hide and seek in the open sea: Pelagic camouflage and visual countermeasures. *Annu. Rev. Mar. Sci.* **6**, 369–392 (2014).
10. S. Johnsen, E. A. Widder, The physical basis of transparency in biological tissue: Ultrastructure and the minimization of light scattering. *J. Theor. Biol.* **199**, 181–198 (1999).
11. T. M. Zaret, Predators, invisible prey, and the nature of polymorphism in the Cladocera (Class Crustacea). *Limnol. Oceanogr.* **17**, 171–184 (1972).
12. T. M. Zaret, W. C. Kerfoot, Fish predation on *Bosmina longirostris*: Body-size selection versus visibility selection. *Ecology* **56**, 232–237 (1975).
13. S. Hylander, M. S. Souza, E. Balseiro, B. Modenutti, L.-A. Hansson, Fish-mediated trait compensation in zooplankton. *Funct. Ecol.* **26**, 608–615 (2012).
14. L. A. Hansson, Induced pigmentation in zooplankton: A trade-off between threats from predation and ultraviolet radiation. *Proc. Biol. Sci.* **267**, 2327–2331 (2000).
15. M. Arias, M. Elias, C. Andraud, S. Berthier, D. Gomez, Transparency improves concealment in cryptically coloured moths. *J. Evol. Biol.* **33**, 247–252 (2020).
16. M. Arias *et al.*, Transparency reduces predator detection in mimetic clearwing butterflies. *Funct. Ecol.* **33**, 1110–1119 (2019).
17. A. Rudh, A. Qvarnström, Adaptive colouration in amphibians. *Semin. Cell Dev. Biol.* **24**, 553–561 (2013).

18. C. Michalis, "Background matching camouflage." PhD thesis, University of Bristol, Bristol, UK (2017).
19. R. H. Siddique, G. Gomard, H. Hölscher, The role of random nanostructures for the omnidirectional anti-reflection properties of the glasswing butterfly. *Nat. Commun.* **6**, 6909 (2015).
20. D. A. Klomp, D. Stuart-Fox, I. Das, T. J. Ord, Gliding lizards use the position of the sun to enhance social display. *Biol. Lett.* **13**, 20160979 (2017).
21. L. J. Fleishman, B. Ogas, D. Steinberg, M. Leal, Why do Anolis dewlaps glow? An analysis of a translucent visual signal. *Funct. Ecol.* **30**, 345–355 (2016).
22. M. Quiroga-Carmona, A. Naveda-Rodríguez, Crested Quetzal (*Pharomachrus antisianus*) preying on a glassfrog (Anura, Centrolenidae) in Sierra de Perijá, northwestern Venezuela. *Ornithol. Res* **22**, 419–421 (2014).
23. J. B. Barnett *et al*, Data for: Imperfect transparency and camouflage in glass frogs. University of Bristol Research Data Repository. https://doi.org/10.5523/bris.3qnujjtjg4v4z2cztb4h882hh3. Deposited 8 March 2020.
24. N. S. Hart, Vision in the peafowl (Aves: *Pavo cristatus*). *J. Exp. Biol.* **205**, 3925–3935 (2002).
25. J. M. Macedonia *et al*., Conspicuousness of Dickerson's collared lizard (*Crotaphytus dickersonae*) through the eyes of conspecifics and predators. *Biol. J. Linn. Soc. Lond.* **97**, 749–765 (2009).
26. J. B. Calderone, G. H. Jacobs, Spectral properties and retinal distribution of ferret cones. *Vis. Neurosci.* **20**, 11–17 (2003).
27. J. B. Barnett, C. Michalis, N. E. Scott-Samuel, I. C. Cuthill, Distance-dependent defensive coloration in the poison frog *Dendrobates tinctorius*, Dendrobatidae. *Proc. Natl. Acad. Sci. U.S.A.* **115**, 6416–6421 (2018).
28. V. C. Smith, J. Pokorny, Spectral sensitivity of the foveal cone photopigments between 400 and 500 nm. *Vision Res.* **15**, 161–171 (1975).
29. D. Bates, M. Mächler, B. M. Bolker, S. Walker, Fitting linear mixed-effects models using lme4. *J. Stat. Softw.* **67**, 1–48 (2014).
30. R Core Team, *R: A Language and Environment for Statistical Computing*, (R Foundation for Statistical Computing, Vienna, 2019).
31. X. Robin *et al*., pROC: An open-source package for R and S+ to analyze and compare ROC curves. *BMC Bioinformatics* **12**, 77 (2011).
32. B. Lantz, *Machine Learning with R*, (Packt Publishing, 2013).
33. T. Troscianko, C. P. Benton, P. G. Lovell, D. J. Tolhurst, Z. Pizlo, Camouflage and visual perception. *Philos. Trans. R. Soc. Lond. B Biol. Sci.* **364**, 449–461 (2009).
34. L. M. Costello, N. E. Scott-Samuel, K. Kjernsmo, I. C. Cuthill, False holes as camouflage. *Proc. Biol. Sci.* **287**, 20200126 (2020).
35. F. Xiao, I. C. Cuthill, Background complexity and the detectability of camouflaged targets by birds and humans. *Proc. Biol. Sci.* **283**, 20161527 (2016).
36. T. Hothorn, F. Bretz, P. Westfall, Simultaneous inference in general parametric models. *Biom. J.* **50**, 346–363 (2008).
37. T. M. Therneau, coxme: Mixed Effects cox Models, R package Version 2.2-5 (2015). Available at: https://cran.r-project.org/web/packages/coxme/index.html. Accessed 6 March 2020.
38. M. Stevens, I. C. Cuthill, Disruptive coloration, crypsis and edge detection in early visual processing. *Proc. Biol. Sci.* **273**, 2141–2147 (2006).
39. R. J. Webster, J.-G. J. Godin, T. N. Sherratt, The role of body shape and edge characteristics on the concealment afforded by potentially disruptive marking. *Anim. Behav.* **104**, 197–202 (2015).
40. M. Stevens, S. Merilaita, Defining disruptive coloration and distinguishing its functions. *Philos. Trans. R. Soc. Lond. B Biol. Sci.* **364**, 481–488 (2009).
41. S. Merilaita, N. E. Scott-Samuel, I. C. Cuthill, How camouflage works. *Philos. Trans. R. Soc. Lond. B Biol. Sci.* **372**, 20160341 (2017).
42. M. Stevens, C. A. Párraga, I. C. Cuthill, J. C. Partridge, T. S. Troscianko, Using digital photography to study animal coloration. *Biol. J. Linn. Soc. Lond.* **90**, 211–237 (2007).
43. J. B. Barnett, N. E. Scott-Samuel, I. C. Cuthill, Aposematism: Balancing salience and camouflage. *Biol. Lett.* **12**, 20160335 (2016).
44. J. B. Barnett, I. C. Cuthill, N. E. Scott-Samuel, Distance-dependent aposematism and camouflage in the cinnabar moth caterpillar (*Tyria jacobaeae*, Erebidae). *R. Soc. Open Sci.* **5**, 171396 (2018).
45. A. Kelber, D. Osorio, From spectral information to animal colour vision: Experiments and concepts. *Proc. Biol. Sci.* **277**, 1617–1625 (2010).
46. M. Vorobyev, D. Osorio, Receptor noise as a determinant of colour thresholds. *Proc. Biol. Sci.* **265**, 351–358 (1998).